Revision 1

Edscottite, Fe_5C_2, a new iron carbide mineral from the Ni-rich Wedderburn IAB iron meteorite

Chi Ma[1,]* and Alan E. Rubin[2,3]

[1]Division of Geological and Planetary Sciences, California Institute of Technology, Pasadena, California 91125, USA

[2]Department of Earth, Planetary, and Space Sciences, University of California, Los Angeles, California 90095-1567, USA

[3]Maine Mineral & Gem Museum
99 Main Street, P.O. Box 500, Bethel, ME 04217, USA

ABSTRACT

Edscottite (IMA 2018-086a), Fe_5C_2, is a new iron carbide mineral that occurs with low-Ni iron (kamacite), taenite, nickelphosphide (Ni-rich schreibersite), and minor cohenite in the Wedderburn iron meteorite, a Ni-rich member of the group IAB complex. The mean chemical composition of edscottite determined by electron probe microanalysis, is (wt%) Fe 87.01, Ni 4.37, Co 0.82, C 7.90, total 100.10, yielding an empirical formula of $(Fe_{4.73}Ni_{0.23}Co_{0.04})C_{2.00}$. The end-member formula is Fe_5C_2. Electron back-scatter diffraction shows that edscottite has the *C*2/*c* Pd_5B_2-type structure of the synthetic phase called Hägg-carbide, χ-Fe_5C_2, which has a = 11.57 Å, b = 4.57 Å, c = 5.06 Å, β = 97.7°, V = 265.1 Å^3, and Z = 4. The calculated density using the measured composition is 7.62 g/cm^3. Like the other two carbides found in iron meteorites, cohenite (Fe_3C) and haxonite ($Fe_{23}C_6$), edscottite forms in kamacite, but unlike these two carbides it forms laths, possibly due to very rapid growth after supersaturation of carbon. Haxonite (which typically forms in carbide-bearing, Ni-rich members of the IAB complex) has not been observed in Wedderburn. Formation of edscottite rather than haxonite may have resulted from a lower C concentration in Wedderburn and hence a lower growth temperature. The new mineral is named in honor of Edward (Ed) R. D. Scott, pioneering cosmochemist at the University of Hawai'I at Manoa, for his seminal contributions to research on meteorites.

Keywords: edscottite, Fe_5C_2, new mineral, iron carbide, Wedderburn iron meteorite.
*E-mail: chi@gps.caltech.edu

INTRODUCTION

The Wedderburn iron meteorite, found as a single 210-g mass in Victoria, Australia in 1951 (Buchwald, 1975), is a Ni-rich ataxite belonging to subgroup sLH of the IAB complex (Low-Au, High-Ni subgroup; Wasson and Kallemeyn, 2002). It was initially classified as group IIID (Buchwald 1975). During a mineralogical re-investigation of a polished thick section of Wedderburn, we identified a new iron-carbide mineral, Fe_5C_2 with the *C2/c* Pd_5B_2-type structure, which we named "edscottite" (Fig. 1). To characterize its chemical composition, structure, and associated phases, we used high-resolution scanning electron microscopy (SEM), electron back-scatter diffraction (EBSD), and electron probe microanalysis (EPMA). This phase was identified chemically as Fe_5C_2 by Scott and Agrell (1971) and described simply as a carbide by Buchwald (1975). Although synthetic Fe_5C_2 is well known (e.g., Hägg 1934; Jack and Wild 1966; Retief 1999; Leineweber et al. 2012), the discovery by Scott and Agrell (1971) prompted us to characterize Fe_5C_2 in Wedderburn as the first natural occurrence of this new carbide mineral.

MINERAL NAME AND TYPE MATERIAL

The new mineral and its name have been approved by the Commission on New Minerals, Nomenclature and Classification of the International Mineralogical Association (IMA 2018-086a) (Ma and Rubin 2019). The mineral name is in honor of Edward (Ed) R. D. Scott (born in 1947), esteemed cosmochemist at the University of Hawai'I at Manoa, USA, for his multifaceted contributions to research on meteorites. He discovered haxonite, $(Fe,Ni)_{23}C_6$ (Scott 1971), as well as this new iron carbide in Wedderburn. The new carbide phase was described as forming plates a few micrometers thick within kamacite (Scott and

Agrell 1971; Scott 1972). The type specimen of edscottite is in Wedderburn polished thick section UCLA 143, housed in the Meteorite Collection of the Department of Earth, Planetary, and Space Sciences, University of California, Los Angeles, California 90095-1567, USA.

APPEARANCE AND OCCURRENCE

Edscottite occurs as subhedral, lath-shaped or platy single crystals, ~0.8 μm × 15 μm to 1.2 μm × 40 μm and 4.0 μm × 18 μm in size, which is the holotype material in thick section UCLA 143 (Fig. 1). The new carbide is commonly associated with small amounts of cohenite and forms in low-Ni iron (known as "kamacite" in the meteorite literature) surrounding grains of nickelphosphide (Ni-rich schreibersite) in a matrix of fine-grained iron (plessite). The mineral appears white microscopically in reflected light. Luster, streak, hardness, tenacity, cleavage, fracture, density, and optical properties were not determined because of the small grain size.

CHEMICAL COMPOSITION

Backscattered electron (BSE) images were obtained at Caltech using a ZEISS 1550VP field emission SEM and a JEOL 8200 electron microprobe with solid-state BSE detectors. Six quantitative WDS elemental microanalyses of type edscottite were carried out using the JEOL 8200 electron microprobe operated at 12 kV (for smaller interaction volume) and 10 nA in focused beam mode. The focused electron beam is ~120 nm in diameter. The interaction volume for X-ray generation in edscottite is ~600 nm in diameter, estimated using the Casino Monte Carlo simulation of electron trajectory. Both the Wedderburn section and the probe standards were uncoated for the probe analyses, following the method of Scott (1972). There is no charging issue. Carbon was measured using Canyon Diablo cohenite ($Fe_{2.96}Ni_{0.04}C$) as a standard. Analyses were processed with the CITZAF correction procedure (Armstrong 1995) using the Probe for EPMA program from Probe Software, Inc. Possible interferences on peak position and background position were checked and corrected for all measured elements based on WDS scans. On-peak interference of Co*Kα* by Fe was corrected using the Probe for EPMA. Analysis of a pure Fe metal standard as an unknown did not show any Co. Analytical results are given in Table 1. Elemental P was also analyzed but was below the detection limit of 0.02 wt% at 99% confidence. WDS scans did not reveal other elements.

The empirical formula of type edscottite (based on 7 atoms *pfu*) is $(Fe_{4.73}Ni_{0.23}Co_{0.04})C_{2.00}$. The end-member formula is Fe_5C_2, which is equivalent to a composition of (in wt%): Fe 92.08, C 7.92.

Associated cohenite has an empirical formula (based on 4 atoms *pfu*) of $(Fe_{2.82}Ni_{0.13}Co_{0.03})C_{1.03}$. Low-Ni iron (kamacite) has a composition of $Fe_{0.93}Ni_{0.06}Co_{0.01}$. Taenite has a composition of $Fe_{0.67}Ni_{0.32}Co_{0.01}$. Nickelphosphide (Ni-rich schreibersite) has an empirical formula (based on 4 atoms *pfu*) of $(Ni_{1.63}Fe_{1.37}Co_{0.01})P_{0.99}$. The fine-grained iron-meteorite matrix has an average composition of $Fe_{0.77}Ni_{0.22}Co_{0.01}$.

CRYSTALLOGRAPHY

Single-crystal electron backscatter diffraction (EBSD) analyses were performed using an HKL EBSD system on a ZEISS 1550VP Field-Emission SEM, operated at 20 kV and 6 nA in focused-beam mode with a 70º tilted stage and in a variable pressure mode (25 Pa). The focused electron beam is several nanometers in diameter. The spatial resolution for diffracted backscattered electrons is ~30 nm in size. The EBSD system was calibrated using a single-crystal silicon standard. The structure was determined and cell constants were obtained by matching the experimental EBSD patterns with the known structures of Fe-C phases, including Fe_3C, Fe_5C_2, Fe_4C, Fe_2C, Fe_7C_3, $(Fe,Ni)_{23}C_6$ and $Fe_{0.96}C_{0.06}$.

The EBSD patterns are indexed only by the *C*2/*c* Pd_5B_2-type structure and are best fit by the synthetic χ-Fe_5C_2 structure of Leineweber et al. (2012) (Fig. 2), in which a = 11.57 Å, b = 4.57 Å, c = 5.06 Å, β = 97.7°, V = 265.1 Å^3, and Z = 4. The mean angular deviation of the patterns is 0.45º - 0.48º. The calculated density based on the empirical formula is 7.62 g/cm^3. Calculated X-ray powder diffraction data are given in Table S1.

Minor cohenite ($Fe_{2.82}Ni_{0.13}Co_{0.03}C$) occurs on the rim and in the interior of edscottite laths, as revealed by EBSD mapping (Fig. 3). Many of the cohenite grains within the edscottite laths are as small as ~150 nm.

DISCUSSION

Formation of edscottite

Edscottite is a new iron-carbide, Fe_5C_2, joining cohenite (Fe_3C) and haxonite ($(Fe,Ni)_{23}C_6$) as a naturally occurring, approved mineral. This phase precipitates in steels where it is called Hägg-carbide (Fang et al. 2010). Its atomic C/Fe ratio (0.40) is appreciably higher than those of cohenite (0.33) or haxonite (0.26). All three phases are among the iron carbides (natural and synthetic) with the lowest enthalpies of formation (ΔH_f) (Fang et al. 2010).

Edscottite has not only been identified in the Wedderburn iron meteorite, one of the most Ni-rich irons known (23.4 wt% Ni; Wasson and Kallemeyn 2002), but also in the Semarkona unequilibrated LL3.0 ordinary chondrite under TEM (Keller 1998). Like cohenite and haxonite, edscottite forms metastably in kamacite, but it differs from cohenite and haxonite in that it occurs as laths, possibly due to very rapid growth after nucleating at the boundaries of kamacite grains.

The edscottite lath in Fig. 1c appears to have nucleated at a kamacite-taenite grain boundary. Because the lath crosses the boundary of adjacent kamacite grains, it must have nucleated before the boundary between the two kamacite grains formed.

Wedderburn is a slowly cooled iron meteorite, like other members of its compositional subgroup. These other irons typically contain haxonite with minor cohenite but lack edscottite (Scott 1972; Buchwald, 1975; Goldstein et al. 2017). In contrast, Wedderburn contains edscottite with minor cohenite but lacks haxonite. Two carbide-containing members of the IAB complex, Freda (sLH subgroup) and San Cristobal, resemble Wedderburn in having high bulk Ni (23 - 25 wt%) and Co (0.6 wt%) (Wasson and Kallemeyn 2002). All three are slowly cooled, Ni-rich ataxites with broadly similar metallographic structures and contain kamacite and taenite grains with similar Ni and Co concentrations. However, the carbide mineralogy in these three irons is not the same: Freda has approximately equal amounts of haxonite and cohenite, San Cristobal contains appreciably more haxonite than cohenite, while Wedderburn contains edscottite with minor cohenite. Buchwald (1975) noted that Freda and San Cristobal, unlike Wedderburn, contain graphite, which formed before the carbides. The laths of edscottite (15 - 40 µm long) in Wedderburn are smaller than carbides in Freda (haxonite up to 100 µm long) or San Cristobal (cohenite up to 50 µm wide) (Buchwald 1975). The small size of the carbides in Wedderburn and the apparent lack of graphite point to lower bulk carbon in Wedderburn. As explained below, this difference and the lath shape of edscottite suggest that the unusual carbide assemblage in Wedderburn may reflect carbide growth at lower temperatures than in Freda and San Cristobal.

The bulk Ni content of a slowly cooled iron meteorite determines when the Fe-Ni system is saturated with C. Wedderburn, with its very high Ni content, does not reach the solvus on the Fe-Ni phase diagram (e.g., Reuter et al. 1989) and become saturated with C until cooling to a relatively low temperature. The nature of the carbide that nucleates and grows also depends on bulk P because kamacite grains nucleate on schreibersite. Wedderburn appears to contain appreciably more bulk P than Freda or San Cristobal (Buchwald 1975).

Nickel concentrations in edscottite and haxonite are similar (3.5 - 5 wt.%) but Co concentrations in haxonite, 0.05-0.4 wt.%, are much lower than in edscottite, which contains ~0.8 wt% Co (Table 1; Scott and Agrell 1971), close to that in kamacite (0.8-1.0 wt.%). It is possible that the lower inferred formation temperature of edscottite favored its growth over that of haxonite; this is because Co diffusion into surrounding kamacite around carbide grains would have been more sluggish at lower temperatures, favoring the more-Co-rich carbide phase. [The diffusion rates for C are many orders of magnitude faster than for Ni and Co (e.g., Goldstein et al. 2017).] This is consistent with the high concentrations of Co (several wt%) in kamacite that is immediately adjacent to haxonite grains in the IAB irons Edmonton (Kentucky) and Freda (E.R.D. Scott, pers. commun., 2019).

Small cohenite grains at the rim and in the interior of edscottite laths (Fig. 3) likely nucleated at the edges of the growing laths in Wedderburn. Edscottite may have reacted with reduced iron from the surrounding kamacite to produce cohenite.

Because shock metamorphism in iron meteorites tends to transform Fe-carbides (which are metastable) into graphite (e.g., as in IIIE irons; Breen et al. 2016), it seems unlikely that

DOI: https://doi.org/10.2138/am-2019-7102

shock played any role in the formation of edscottite. In addition, Wedderburn is an unshocked iron (Buchwald 1975) and graphite was not observed in the section.

<u>Other occurrences of Fe carbide</u>

Iron carbides have also been observed in other meteorites: e.g., ureilites (Goodrich et al. 2013, 2014), type-3 ordinary chondrites (Taylor et al., 1981; Krot et al., 1997; Keller, 1998) and CO3 chondrites (Scott and Jones, 1990; Simon et al., 2019). There are several terrestrial occurrences of iron carbides. Kaminsky and Wirth (2011) reported cohenite, haxonite and Fe_2C ("chalypite") in Brazilian diamonds derived from the lower mantle. Goodrich and Bird (1985) described cohenite in native iron masses derived from a C-bearing mafic silicate melt in Disko Island, West Greenland. Although edscottite has not been previously observed, computational studies of Earth's inner core show that the most stable iron carbides are Fe_3C, Fe_7C_3 and Fe_2C; edscottite (along with Fe_4C) is close to stability at these high pressures (~350 GPa; Weerasinghe et al. 2011) and might be present.

IMPLICATIONS

Wedderburn is a slowly cooled, Ni-rich iron meteorite that appears to have reached C supersaturation at a lower temperature than other irons due in part to a lower bulk C concentration. These conditions facilitated the rapid growth of edscottite laths within low-Ni iron (kamacite). Iron carbides (cohenite and haxonite) in other iron meteorites do not form laths and appear to have grown more slowly and at somewhat higher temperatures. Edscottite may be restricted to slowly cooled Ni-rich iron meteorites like Wedderburn.

ACKNOWLEDGMENTS

We thank Ed Scott for discussions and insightful comments. Optical microscopy was done at UCLA and Caltech. SEM, EBSD and EPMA were carried out at the Geological and Planetary Science Division Analytical Facility, Caltech, which is supported in part by NSF grants EAR-0318518 and DMR-0080065. This work was also supported by NASA grants NNX15AH38G and NNG06GF95G. We thank Alex Ruzicka, Cyrena Goodrich and Tim McCoy for their constructive reviews.

REFERENCES CITED

Armstrong, J.T. (1995) CITZAF: A package of correction programs for the quantitative electron beam X-ray analysis of thick polished materials, thin films, and particles. Microbeam Analysis, 4, 177–200.

Breen, J.P., Rubin, A.E., and Wasson, J.T. (2016) Variations in impact effects among IIIE iron meteorites. Meteoritics and Planetary Science, 51, 1611–1631.

Buchwald, V. F. (1975) *Handbook of Iron Meteorites*. University of California Press, Berkeley, CA. Available in electronic form at http://evols.library.manoa.hawaii.edu/handle/10524/33750.

Fang, C.M., Sluiter, M.H.F., van Huis, M.A., Ande, C.K., and Zandbergen, H.W. (2010) Origin of predominance of cementite among iron carbides in steel at elevated temperature. Physical Review – Letters, 105, 055503.

Goodrich, C.A. and Bird, J.M. (1985) Formation of Iron-Carbon alloys in basaltic magma at Iivfaq, Disko Island: The role of carbon in mafic magmas. Journal of Geology, 93, 475–492.

Goodrich, C.A., Ash, R.D., Van Orman, J.A., Domanik, K., and McDonough, W.F.. (2013) Metallic phases and siderophile elements in main group ureilites: Implications for ureilite petrogenesis. Geochimica et Cosmochimica Acta, 112, 340–373.

DOI: https://doi.org/10.2138/am-2019-7102

Goodrich, C.A., Harlow, G.E., Van Orman, J.A., Sutton, S.R., Jercinovic, M.J., and Mikouchi, T. (2014) Petrology of chromite in ureilites: Deconvolution of primary oxidation states and secondary reduction processes. Geochimica et Cosmochimica Acta, 135, 126–169.

Goldstein, J. I., Huss, G.R., and Scott, E.R.D. (2017) Ion microprobe analyses of carbon in Fe-Ni metal in iron meteorites and mesosiderites. Geochimica et Cosmochimica Acta, *200,* 367–407.

Hägg, G. (1934) Pulverphotogramme eines neuen Eisencarbides. Zeitschrift für Kristallographie - Crystalline Materials, 89, 92–94.

Jack, K.H. and Wild, S. (1966) Nature of χ-carbide and its possible occurrence in steels. Nature, 212, 248–250.

Kaminsky, F.V. and Wirth, R. (2011) Iron carbide inclusions in lower-mantle diamond from Juina, Brazil. Canadian Mineralogist, 49, 555–572.

Keller, L.P. (1998) A transmission electron microscope study of iron-nickel carbides in the matrix of the Semarkona unequilibrated ordinary chondrite. Meteoritics & Planetary Science, 33, 913–919.

Krot, A. N., Zolensky, M. E., Wasson, J. T., Scott, E. R. D., Keil K. and Ohsumi, K. (1997) Carbide-magnetite assemblages in type-3 ordinary chondrites. Geochim. Cosmochim. Acta, 61, 219-237.

Leineweber, A., Shang, S., Liu, Z., Widenmeyer, M., and Niewa, R. (2012) Crystal structure determination of Hägg carbide, χ-Fe_5C_2 by first-principles calculations and Rietveld refinement. Zeitschrift für Kristallographie - Crystalline Materials, 227, 207–220.

Ma, C. and Rubin, A. (2019) Edscottite, IMA 2018-086a. CNMNC Newsletter No. 47, February 2019: 204. European Journal of Mineralogy, 31, 199–204.

Retief, J.J. (1999) Powder diffraction data and Rietveld refinement of Hägg-carbide, χ-(Fe_5C_2). Powder Diffraction, 14, 130–132.

Reuter, K.B., Williams, D.B., and Goldstein, J.I. (1989) Determination of the Fe-Ni phase diagram below 400ºC. Metallurgical Transactions A, 20, 719–725.

Scott, E.R.D. (1971) New carbide, $(Fe,Ni)_{23}C_6$, found in iron meteorites. Nature, 229, 61–62.

Scott, E.R.D. (1972) Geochemistry, mineralogy and petrology of iron meteorites. Ph.D. thesis of University of Cambridge.

This is a preprint, the final version is subject to change, of the American Mineralogist (MSA)
Cite as Authors (Year) Title. American Mineralogist, in press.
DOI: https://doi.org/10.2138/am-2019-7102

Scott E.R.D. and Agrell, S.O. (1971) The occurrence of carbides in iron meteorites (abstract). Meteoritics, 6, 312–313.

Scott, E. R. D. and Jones, R. H. (1990) Disentangling nebular and asteroidal features of CO3 carbonaceous chondrite meteorites. Geochim. Cosmochim. Acta, 54, 2485-2502.

Simon, S. B., Sutton, S. R., Brearley, A. J., Krot, A. N. and Nagashima, K. (2019) The effects of thermal metamorphism as recorded in CO3.0 through CO3.2 chondrites. Lunar Planet. Sci., 50, abstract#1444.

Taylor, G. J., Okada, A., Scott, E. R. D., Rubin, A. E., Huss, G. R. and Keil, K. (1981) The occurrence and implications of carbide-magnetite assemblages in unequilibrated ordinary chondrites (abstract). Lunar Planet. Sci., 12, 1076-1078.

Wasson, J.T. and Kallemeyn, G.W. (2002) The IAB iron-meteorite complex: A group, five subgroups, numerous grouplets, closely related, mainly formed by crystal segregation in rapidly cooling melts. Geochimica et Cosmochimica Acta, 66, 2445–2473.

Weerasinghe, G.L., Needs, R.J., and Pickard, C.J. (2011) Computational searches for iron carbide in the Earth's inner core. Physical Review B, 84, 174110.

DOI: https://doi.org/10.2138/am-2019-7102

Table 1. Average elemental composition of six point EPMA analyses for type edscottite.

Constituent	wt%	Range	SD	Probe Standard
Fe	87.01	85.90-88.14	0.87	Fe metal
Ni	4.37	3.46-5.02	0.65	Ni metal
Co	0.82	0.80-0.84	0.02	Co metal
C	7.90	7.61-8.21	0.25	cohenite
Total	100.10			

DOI: https://doi.org/10.2138/am-2019-7102

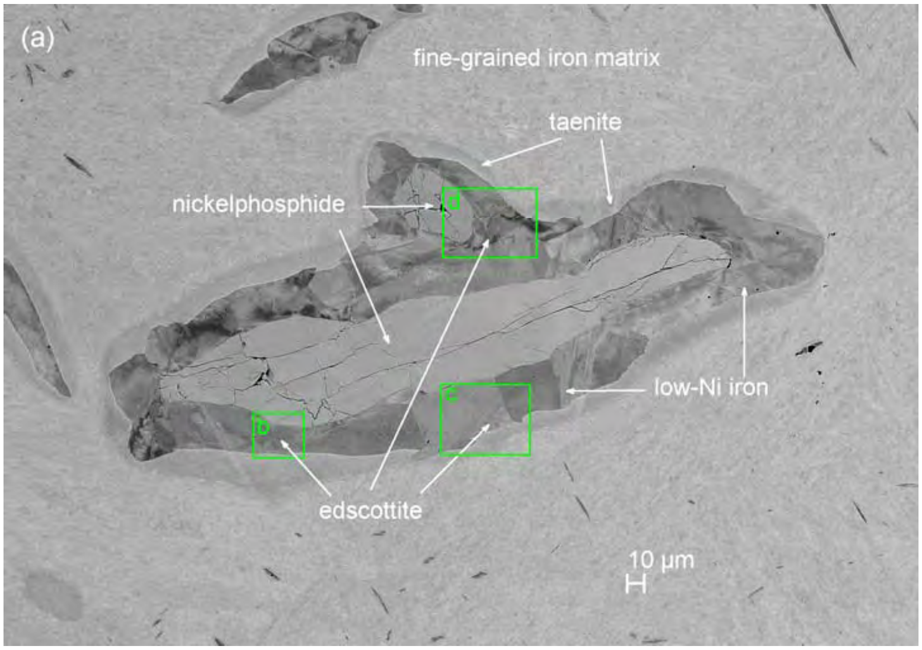

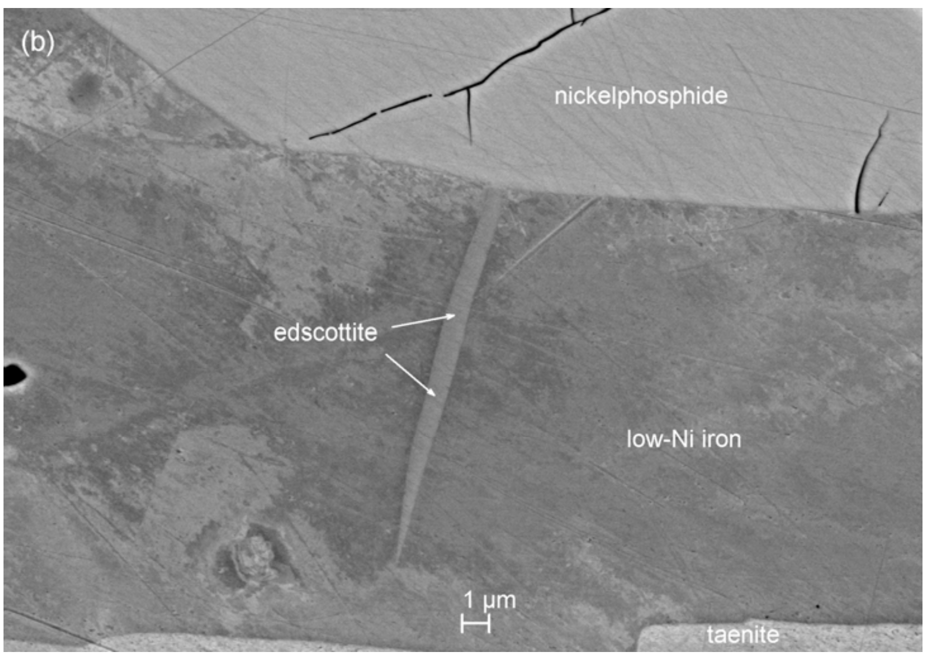

This is a preprint, the final version is subject to change, of the American Mineralogist (MSA)
Cite as Authors (Year) Title. American Mineralogist, in press.
DOI: https://doi.org/10.2138/am-2019-7102

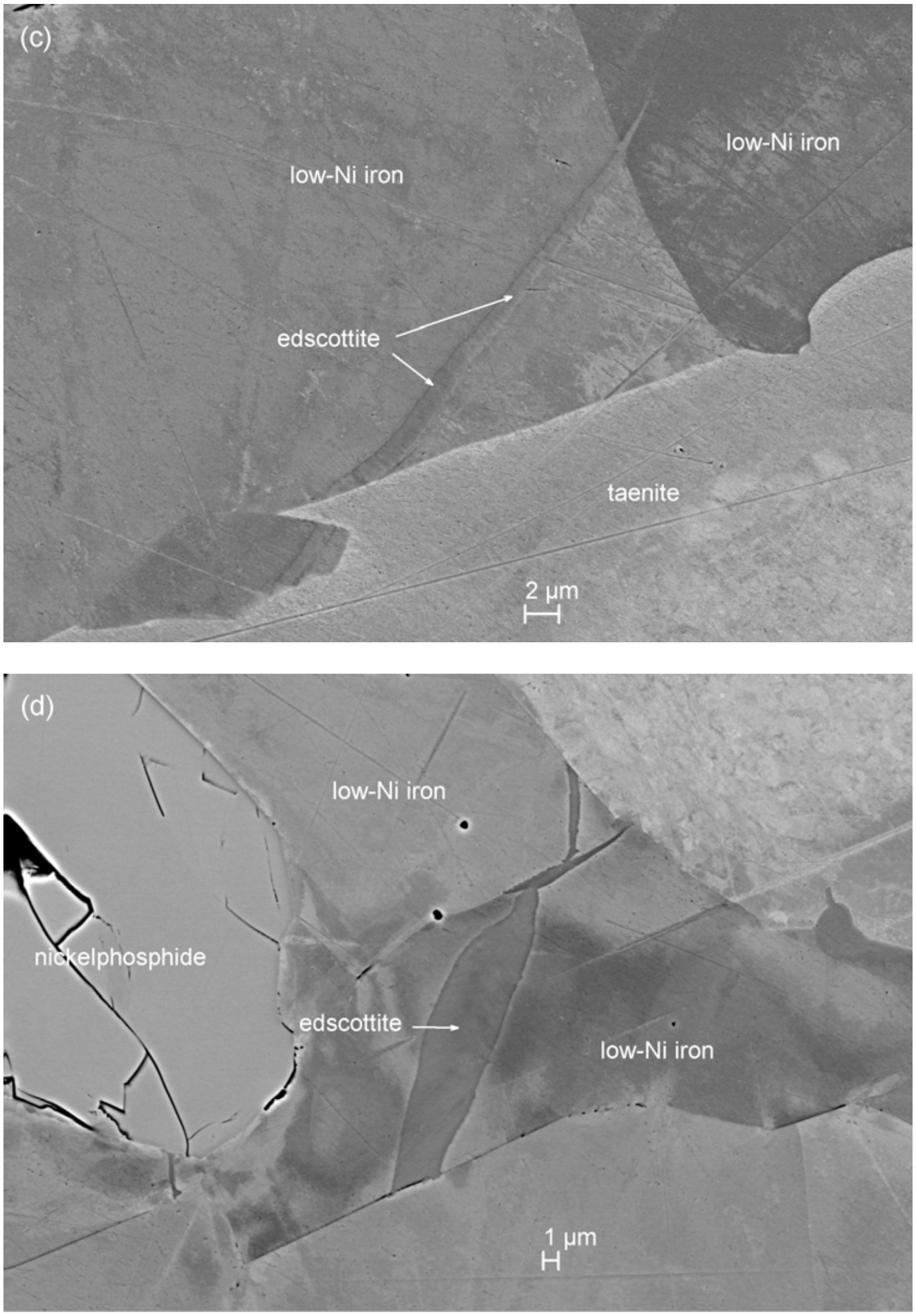

Figure 1. SEM BSE images showing edscottite with taenite, low-Ni iron and nickelphosphide, in the polished Wedderburn section UCLA 143. (a) Overview. (b), (c) and (d) Enlarged BSE images of rectangular regions outlined in panel a.

DOI: https://doi.org/10.2138/am-2019-7102

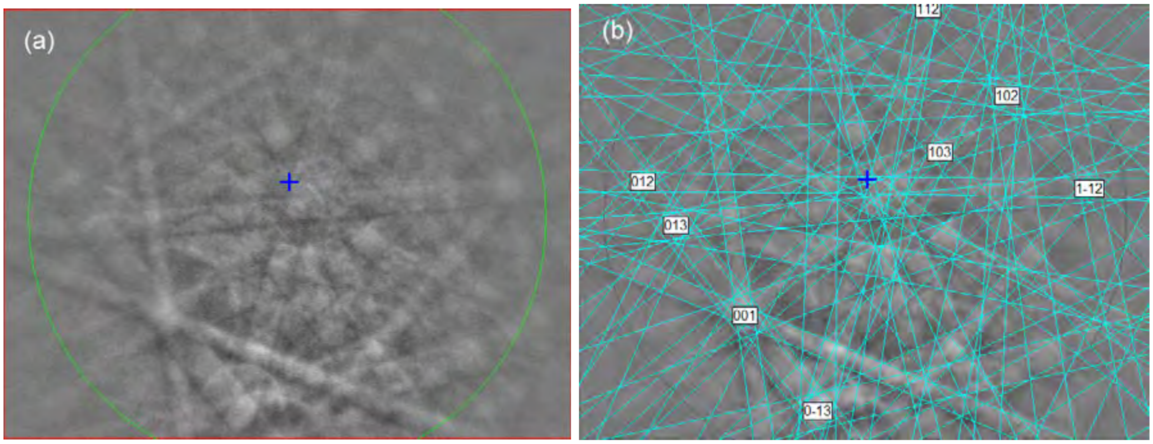

Figure 2. (a) EBSD pattern of one edscottite crystal in Fig. 1, and (b) the pattern indexed with the $C2/c$ Fe_5C_2 structure.

DOI: https://doi.org/10.2138/am-2019-7102

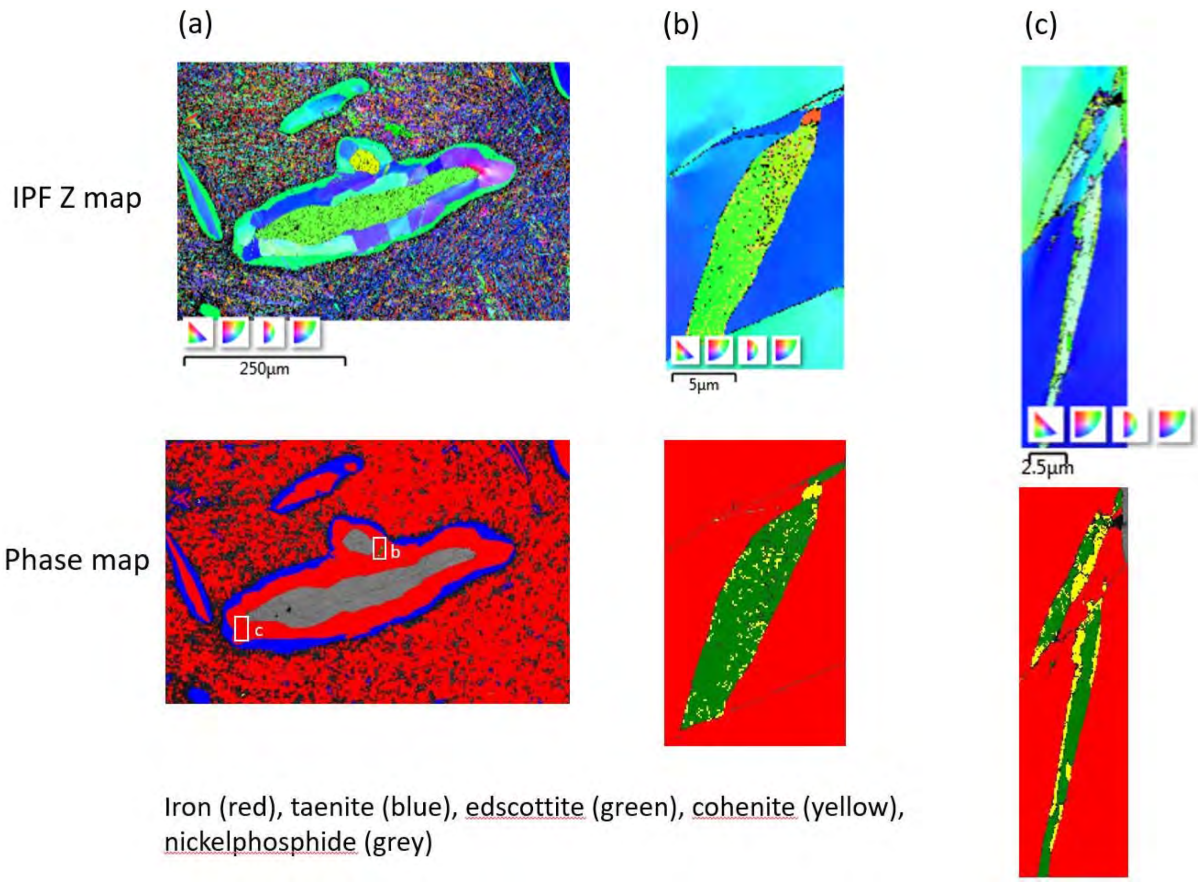

Figure 3. EBSD mapping. (a) The area corresponds roughly to Fig. 1a. Two rectangles in its phase map outline regions in (b) and (c). (b) A region corresponding roughly to Fig. 1d and (c) another region showing cohenite along with edscottite. Top raw: inverse pole figure (IPF) Z orientation maps; bottom raw: phase maps.